Two-Electrode Solar Water Splitting

Permitting H_2 Separation at a Dark Cathode

By Hironobu Ozawa and Ken Sakai

https://doi.org/10.51167/acm00027

Hironobu Ozawa
Hironobu Ozawa received his Ph.D. from Kyushu University in 2007, working under the supervisiory of Prof. Ken Sakai. He carried out his Postdoctoral research in Prof. Koji Tanaka's group at Institute for Molecular Science, Prof. Garry S. Hanan's group at University of Montreal, and Prof. Ken Sakai's group at Kyushu University. In 2010, he became an Assistant Professor at Tokyo University of Science (Prof. Hironori Arakawa's group). In 2015, he moved to Kyushu University as an Assistant Professor (Prof. Ken Sakai's group), and in 2018 he was promoted to an Associate Professor at the Department of Chemistry, Faculty of Science, Kyushu University. His current research interests are focused on the development of solar energy conversion systems based on coordination compounds.

Ken Sakai
Ken Sakai received his Ph.D. from Waseda University in 1993 where he initiated his ongoing study on the hydrogen evolution reaction catalyzed by platinum(II) complexes. He extended his study in the related areas at both Seikei University (1991-1999) and Tokyo University of Science (1999-2004), and was finally promoted to be a full professor at the Department of Chemistry of Kyushu University in 2004. His interests involve the development of hybrid materials for artificial photosynthesis together with the detailed mechanic studies on the dark and photochemical catalysis relevant to the energy conversion processes, such as water splitting and CO2 reduction. He has also been proving his volunteer services to the IUPAC activity as one of the elected members of Bureau (2018-2025).

We want to develop an artificial photosynthetic water splitting device enabling separate evolution of H_2 and O_2 in two different aqueous phases. This approach avoids the evolution of a potentially explosive H_2/O_2 gas mixture together with development of a gas separation facility required to capture H_2 from the mixture. We are thus attempting to develop a two-electrode system for solar-light water splitting with the anode only subjected for photo-driven water oxidation to uptake electrons and protons, as the nature does. Our target device converts the electrons transferred to the cathode directly to H_2 without light illumination, as is the case for the Calvin cycle where CO_2 is converted into glucose as a dark reaction. An outstanding feature also lies in the high specific surface areas of both electrodes due to the mesoporous nature of the TiO_2 films adopted as the electrode materials.

Why hydrogen and other fuel cells rather than battery?

Among various approaches attempting to develop renewable energy sources, solar hydrogen production via water splitting has received an increasing attention in recent years.[1] It actually has a great relevance to the recent advancement in the hydrogen fuel cell technology. The fuel cell electric vehicles (FCEVs) possess several important characteristics superior to the battery electric vehicles (BEVs),[1] even though the FCEVs still suffer from the drawbacks arising from their high costs together with the lack of sufficient numbers of refueling stations. However, the pressurized hydrogen fuel (over 35 MPa)[2] has a higher energy density than lithium-ion batteries, featuring the FCEVs superior to any other zero-emission vehicles for long-distance transportation. Especially, transportation of

heavy materials or a larger number of people by trucks or buses is not a realistic target for the BEVs but is considered achievable by the FCEVs. Moreover, the time required to refuel the FCEVs is short enough and comparable to the gasoline-powered vehicles, representing their high advantages in comparison with the BEVs. In addition, the fuel-to-electricity conversion efficiency over 60% already achieved by the hydrogen fuel cells[3] makes them promising technologies towards the development of a hydrogen energy society.

How we separate the fuels yielded in artificial photosynthesis?

Currently, the mid-term direction rather concentrates on the hydrogen production based on natural gas reforming (i.e., steam methane reforming) together with the innovative technologies permitting the higher energy conversion efficiency as well as the capture, utilization and storage of the CO_2 evolved in the reforming process.[4,5] However, the long-term direction must be focused on the truly renewable energy cycles based on the storable fuels given by reduction of either water or CO_2. For some simplest renewable fuels, the combustion energy averaged for storing two reductive equivalents (i.e., *via* 2-electron reduction) decreases in the order of H_2 (**he**) > CO (0.99**he**), HCHO (0.99**he**) > HCOOH (0.89**he**) > CH_3OH (0.85**he**) > CH_4 (0.78**he**), where **he** denotes the combustion energy of H_2 (286 kcal/mol). Only formic acid and methanol are liquid and possess superior characteristics from a viewpoint of energy density together with the feasibility in refueling and transportation in ambient conditions. Furthermore, formic acid has a remarkable potential as a source of H_2 because of its reversible conversion capability: HCOOH ↔ H_2 + CO_2 (ΔG = -11.6 kcal/mol).[6] There are several ways of converting solar energy into H_2, CO, and HCOOH based on the simple 2-electron reduction (Figure 1, a-c). For all cases, the source of electrons and protons can be produced in the artificial photosynthetic water oxidation process ($2H_2O \rightarrow O_2 + 4H^+ + 4e^-$). Without saying, it is important to separately develop some highly efficient water oxidation catalysts (WOCs).[7] What are the forms of products in each case? In the gaseous fuel production, *flammable* or *explosive* gaseous mixture, {$2H_2$+O_2} or {2CO+O_2}, is yielded, inevitably requiring the extra costs and energy in the gas separation processes.[8] In this context, a two-phase gas evolution system, discussed below, has a great advantage. The photosynthetic production of the {O_2+2HCOOH} mixture (Figure 1c) is also advantageous owing to the spontaneous separation of the two products into the gas and aqueous phases. Moreover, substantial efforts have been made to produce *high pressure hydrogen* based on the catalytic conversion of HCOOH into the {*high-pressure* H_2 + *supercritical* CO_2} mixture within a pressure-resistant vessel having a limited volume (Figure 1d).[9,10] This is a promising way to avoid the use of a mechanical compressor which consumes electrical energy during its operation (Figure 1f). In addition, desirable methods of handling the reverse process, i.e., the catalytic hydrogenation of CO_2 into HCOOH (Figure 1e), must be advanced in order to facilitate the large-scale transportation of hydrogen energy in a liquid form.

The above fuel generation processes combined with water oxidation catalysis may be driven using sustainable energy sources, such as solar, hydroelectric, oceanic, geothermal, wind and so forth. If we limit our discussion on the solar-driven artificial photosynthesis, oxidative and reductive equivalents required to drive the two catalytic processes must be generated *via* the light-harvesting of molecular and/or semiconductor systems.[11-16]

Molecular platinum(II)-based complexes as catalysts for hydrogen evolution reaction.

One of our interests over the last two decades has concentrated on the basic and applied chemistry of molecular hydrogen evolution reaction (HER) catalyzed by various platinum(II) complexes.[17] The study was originally evoked in the late 1980s by finding the HER catalyzed by several *cis*-diammineplatinum(II) dimers doubly bridged by amidate ligands, $[Pt(II)_2(NH_3)_4(\alpha\text{-amidate})_2]^{2+}$ (amidate = α-pyrrolidonate, α-pyridonate, acetamidate, 2-fluoroacetamidate, etc.) (Figure 2).[18-20] In the earlier studies, their catalytic activity was scrutinized using a multi-component system comprising of $[Ru(bpy)_3]^{2+}$ (bpy = 2,2'-bipyridine) as a photosensitizer (**PS**), methylviologen (N,N'-dimethyl-4,4'-bipyridinium; MV^{2+}) as an electron relay (**Accepter**), a platinum(II) complex as a water reduction catalyst (**WRC**), and EDTA·2Na (ethylenediaminetetraaceticacid disodium salt) as a sacrificial electron donor (**Donor**) (Figure 2). For many years, we insisted in studying all catalysts under a common aqueous acetate buffer condition (pH=5.0) in which the driving force for the HER driven by $MV^{+\bullet}$ is only 150 meV. One of the most highly active catalysts (i.e., colloidal platinum) indeed works well so that the exploration of molecular catalysts active with this condition was believed to be the ideal target. The environmentally friendly aqueous conditions free on organic solvents were also considered to be the most suitable conditions when it happens to transfer the technology to the practical applications. Consequently, the Pt(II)-based catalysts had been for a long time the sole family of catalysts active under this condition until we reported on the second and third family of catalysts in 2010s, i.e., carboxylate-bridged dirhodium(II) catalysts[21] and a cobalt-NHC catalyst.[22] The specific features of the $Pt(II)_2$ dimers are represented by the short bridged Pt(II)-Pt(II) distance (ca. 2.8-3.0 Å) together with the air-oxidizable metal centers displaying a quasi-reversible two-electron one-step $Pt(II)_2/Pt(III)_2$ redox couple at *ca.* 0.4-0.6 V vs. SCE,[23] which can also be correlated with the blue and red chromophores in the mixed-valence tetranuclear $Pt(2.25+)_4$ and $Pt(2.5+)_4$ systems given by the stack of dimers. The subsequent studies on various mono- and dinuclear complexes suggested that the metal-metal interaction plays a

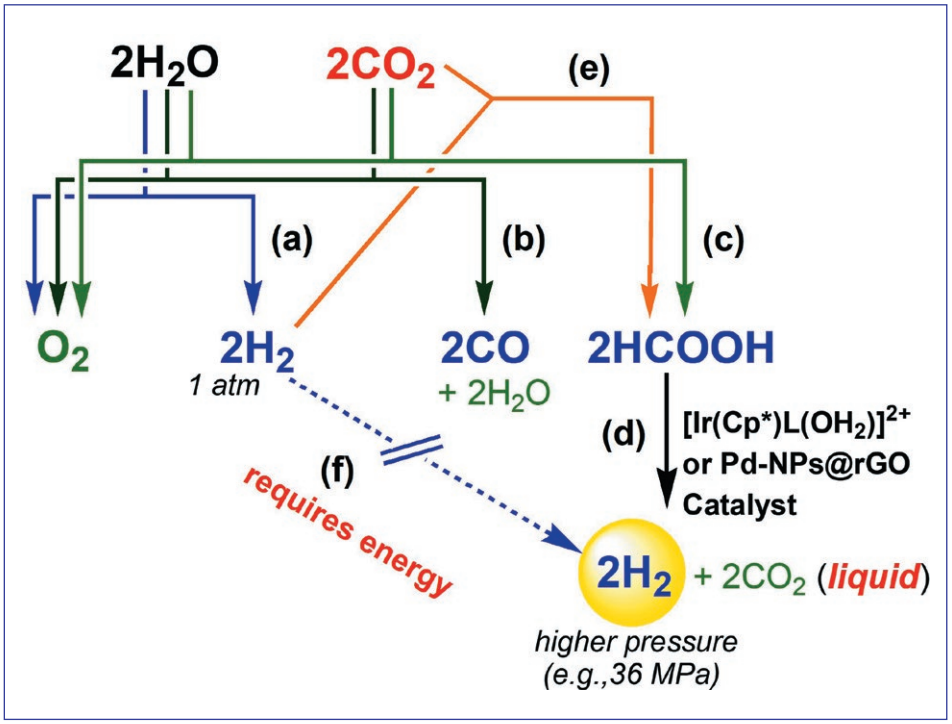

Figure 1. Handling the 2-electron-reduced fuels towards applications in renewable energy cycles.

none-negligible role in the catalytic enhancement.[24-27] These studies provided various experimental and theoretical evidences supporting our conclusion that the Pt(II)-catalyzed H_2 evolution is often accelerated via formation of a hydridodiplatinum(II,III) intermediate: 2Pt(II) + H^+ + e^- —> Pt(II)-Pt(III)-H. The stabilization of this intermediate has been interpreted in terms of the enhanced basicity of the electron pair in the filled Pt(II) d_{z2} orbital because of destabilization at the $\sigma^*(d_{z2}$-$d_{z2})$ antibonding orbital by the stack of two square-planar Pt(II) units. The high HER activity initially found for the amidate-bridged $Pt(II)_2$ dimers may be similarly explained. As noted earlier,[17] the hydride formation accompanies the formal oxidation at the metal center (i.e., $Pt(II)_2$ → $Pt(2.5+)_2$ + e^-) and therefore the strongly donating property of ligands together with the filled-filled d_{z2}-d_{z2} interaction greatly contributes to the thermodynamic stability of the Pt(II)-Pt(III)-H intermediate. Several other groups have so far reported on the results consistent with our conclusion.[28]

On the other hand, we also attempted to develop the dyads and triads constructed by the covalent linkage of components selected from **WRC**, **PS**, **Acceptor**, and **Donor**.[29-32] The first successful model was a **PS-WRC** dyad given by the amide coupling of $[Ru(bpy)_2(5$-amino-phen$)]^{2+}$ (phen = 1,10-phenanthroline) and $PtCl_2$(dcbpy) (dcbpy = 4,4'-dicarboxy-bpy) (Figure 2),[24] which was turned out to be the first example of a *photo-hydrogen-evolving molecular device* promoting the water reduction to H_2 in the presence of **Donor** (EDTA) without any additional components. Based on the photocatalysis experiments combined with the *in-situ* dynamic light scattering (DLS) measurements, the lack of colloidal platinum formation was clearly evidenced for many of such molecular devices developed in our group.[25,30,31,33]

Developing PECs with a dark cathode rather than Tandem PECs

As mentioned above, the two-phase gas evolution technique adopted in our molecular-based photoelectrochemical cells (PECs) has a great advantage (Figure 3c). The original concept was developed by Fujishima and Honda in 1972 (Figure 3a).[11] In their report, a TiO_2 electrode, corresponding to an n-type semiconductor (SC), was irradiated by visible light to evolve O_2 and H_2 at the photoanode (TiO_2) and the dark cathode (Pt), respectively, without applying external bias with the two compartments separated by a glass frit (Figure 3a). They also pointed out that the photoirradiation at the cathode by replacing Pt by a p-type SC should result in more efficient water splitting. By following this concept, the molecular-based PECs with both electrodes subjected for light illumination are intensively studied for overall water splitting in recent years.[34-37] Typically, such PECs consist of a photoanode modified with PS and WOC and a photocathode similarly modified with PS and WRC (Fig. 3b). These PECs are thus classified as Tandem PECs, where TiO_2, SnO_2, WO_3 or $BiVO_4$ (n-type SC) is adopted in the photoanode, while NiO, p-Si or p-GaP (p-type SC) is used in the photocathode. The word "tandem" denotes that two photosensitizers are connected in a tandem fashion in order to successively transfer a single electron based on twice of one-photon pumping. It means that two photons are required for the overall one-electron transfer. Theoretically, at least 8 photons must be absorbed to split water: $2H_2O + 8h\nu \rightarrow 2H_2 + O_2$, leading to the value of 50% in the highest attainable quantum efficiency for the overall photoreaction with this Tandem PECs. Some researchers misleadingly define that "Tandem" is equivalent to the "Z-scheme in oxygenic photosynthesis by green plants (PS-II and PS-I drive water oxidation and NADPH production, respectively)". However, this is not the case because NADPH is not the only photoproduct. More importantly, the electron transport chain connecting the PS-II and PS-I generates the proton gradient energy across the *Thylakoid* membrane which is used to mechanically drive the ATP synthase. To keep the value of 100% regarded as the standard theoretical maximum for the quantum efficiency of photoreactions, our

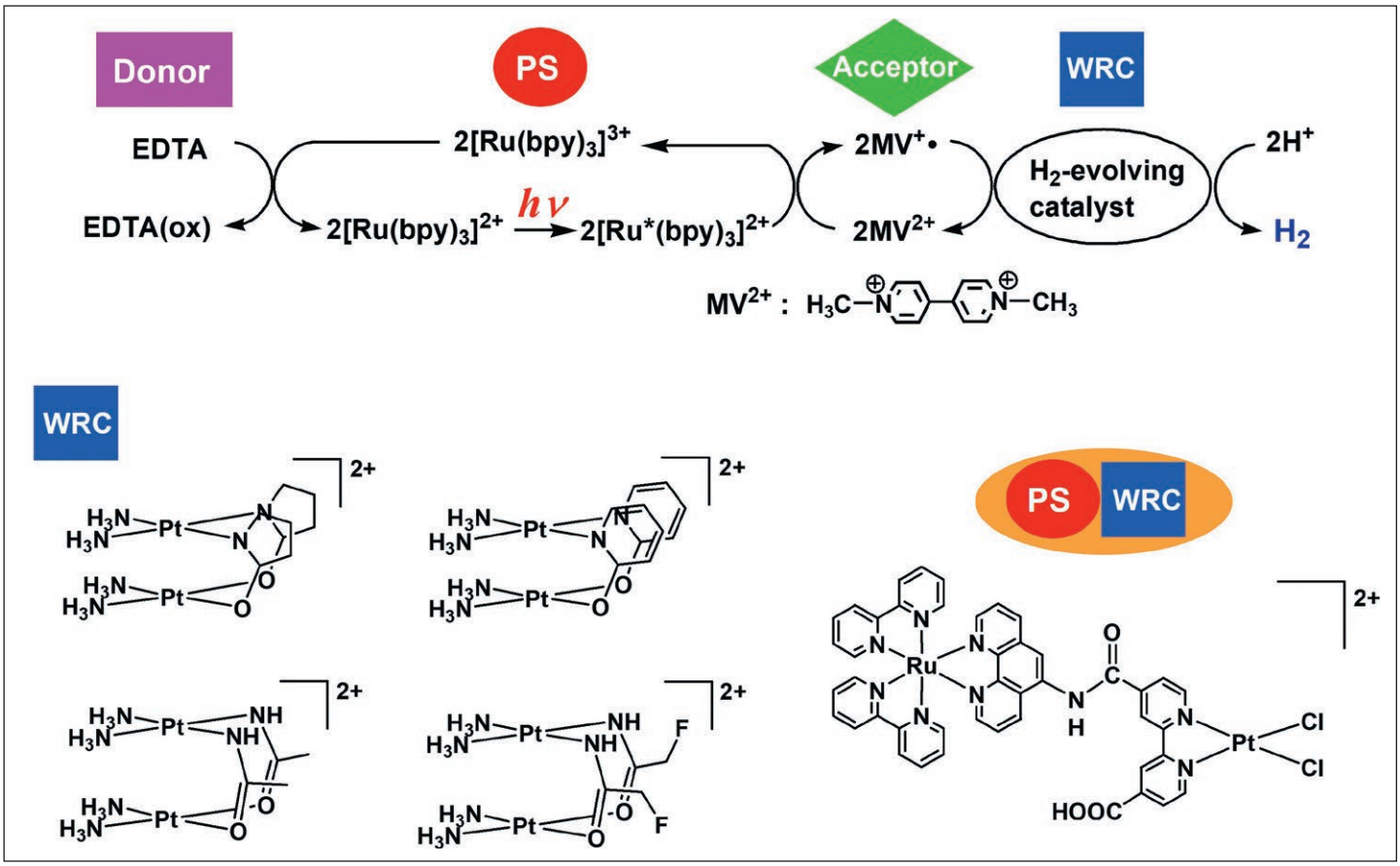

Figure 2. Schematic representation of multi-component system for photochemical HER, and molecular structures of the $Pt(II)_2$ dimers (WRC) together with the dinuclear Ru-Pt photocatalyst (PS-WRC dyad).

PECs (Figure 3c) intend to drive the cathode reaction (HER) in the dark because of the much faster rate generally achieved for the HER compared to the OER (oxygen evolution reaction). In other words, the OER must be considered as a bottleneck in water splitting so that the overpotential required for the OER must be drastically controlled by finely tuning the redox properties of the PS together with the catalytic performance of WOCs in our photoanodes.

Why mesoporous TiO_2 films? Why pyridyl anchors for stable adsorption?

The advancement of our projects on the molecular-based PECs largely relies on the knowledge and experimental techniques gained from the studies on dye-sensitized solar cells (DSSCs).[38] We assume that mesoporous TiO_2 films possess extremely high specific surface area (ca. 80 m^2/g),[39] extremely larger than the apparent film area, and thereby permit the development of practically effective molecular-based PECs exhibiting relatively high hydrogen production capacity. Our initial effort was devoted to invent a new technique to produce tightly anchored molecular PECs which do not easily desorb the molecular components upon soakage into aqueous photolysis solutions. Both carboxylate and phosphonate anchors (Figure 4a,b) are widely adopted in making adsorption of polypyridyl ruthenium dyes and subcomponents in DSSCs, for they are relatively stable anchors in acetonitrile solvent adopted. However, these anchors rather easily dissociate from the TiO_2 surfaces due to the hydrolysis in aqueous media when adopted for the artificial photosynthetic purposes, as described elsewhere.[40] In general, such dyes are highly soluble in water, which also contributes to the rapid desorption of dyes from the TiO_2 surfaces. To substantially suppress desorption of molecular components, we decided to utilize pyridyl anchors (Figure 4c). This *pyridyl anchoring technique* was evoked by a report on DSSCs which revealed improvement in cell performance based on the enhanced co-adsorption of two components using both carboxylate and pyridyl anchors.[41] To test our idea, we initially developed a PEC consisting of a dye-anchored photoanode and a dark platinum cathode (Figure 5).[42] The TiO_2-based photoanode was modified with $[Ru(dmbpy)_2(qpy)]^{2+}$ (**Ru-dmqpy**; dmbpy = 4,4′-dimethyl-2,2′-bipyridine, qpy = 4,4′:2′,2″:4″,4‴-quarterpyridine) having two pyridyl anchors. By illuminating the photoanode by visible light in the presence of sacrificial **Donor** (EDTA), we could successfully demonstrate the stable adsorption of **Ru-dmqpy** over the TiO_2 surfaces in aqueous media by monitoring the sustained evolution of H_2 from the dark cathode. This behavior was also compared with the rapid deactivation of the PEC prepared by using a similar polypyridyl ruthenium dye possessing either carboxylate or phosphonate anchors instead of pyridyl anchors.[42] Importantly, the H_2 evolution was found to proceed even without applying any external bias, in line with our direction to avoid the Tandem type PECs (Figure 5).

Platinum(II)-based HER catalyst anchored to the cathode.

In spite of the superior zero-overpotential characteristics of the HER catalyzed by the platinum electrode, there has been a continued demand to develop comparably efficient non-precious metal HER catalysts for the sake of improving the cost effectiveness. However, as noted above, molecular catalysts capable of promoting the HER under the low driving-force conditions (150 meV by $MV^{+\bullet}/MV^{2+}$) are quite

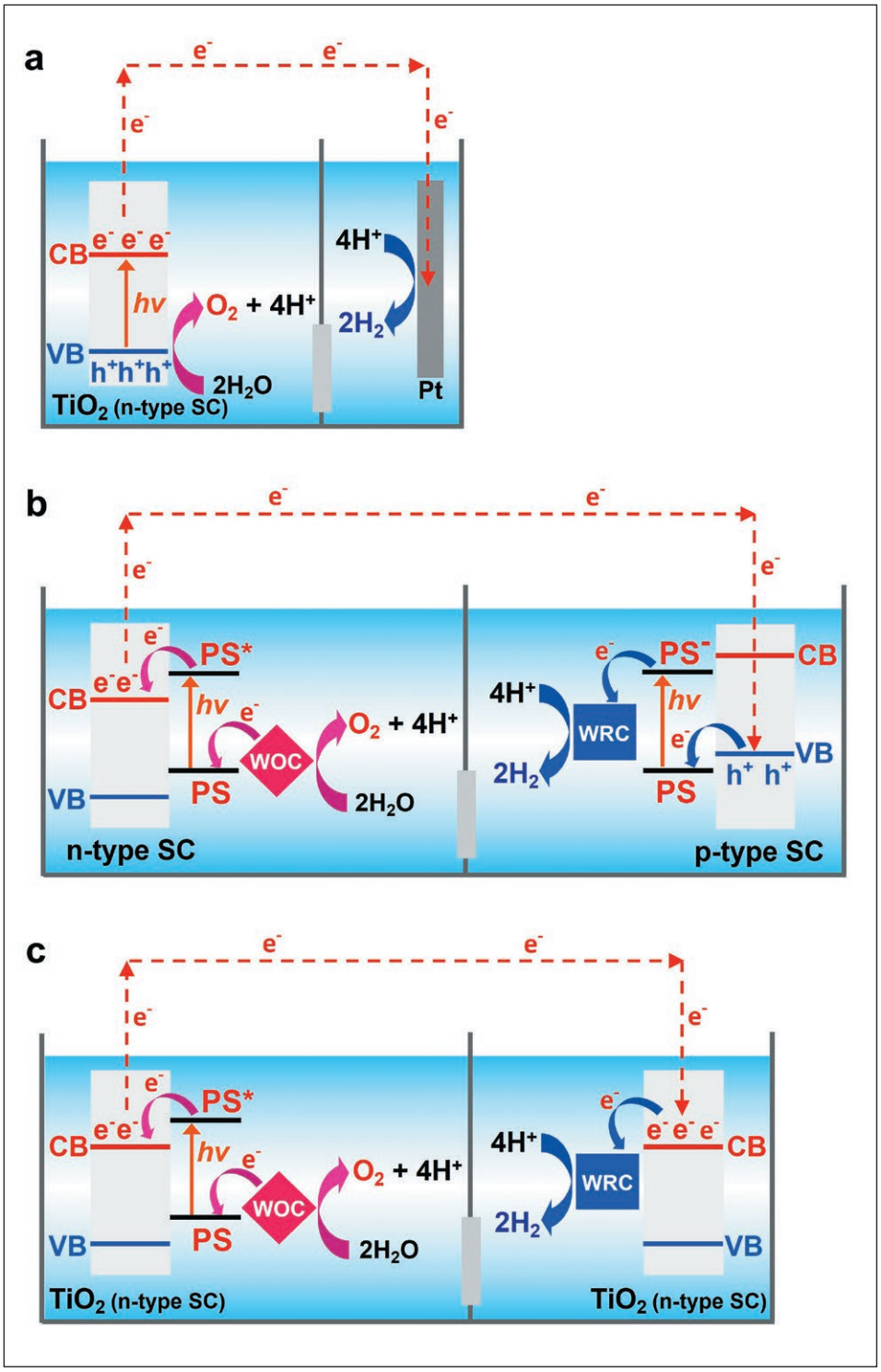

Figure 3. Schematic representation of the PEC reported by Honda and Fujishima (a), tandem PECs (b), and PECs developed by the authors' group (c).

limited. Stability of molecular catalysts tends to become lower under the strong light illumination so that attention should also be paid to the stable ligand frameworks. In addition, molecular motifs having pyridyl anchor(s) showing relatively low solubility in water must be explored as a desirable target to be tightly anchored over the mesoporous TiO_2 cathode surfaces. After our efforts, a platinum porphyrin having a single pyridyl anchor (**PtP-py**) was found to fulfill all these requirements (Figure 6).[43] In the study, $[Ru(dpbpy)_2(qpy)]^{2+}$ (**Ru-dpqpy**; dpbpy = 4,4′-diphenyl-2,2′-bipyridine), possessing a higher hydrophobicity with stabler adsorption characteristics, was also used to improve the photoanode performance. The TiO_2-based photoanode (FTO/TiO_2/**Ru-dpqpy**) and the TiO_2-based cathode (FTO/TiO_2/**PtP-py**) were prepared by submersing the pristine FTO/TiO_2 electrodes into the solutions of **Ru-dpqpy** and **PtP-py**, respectively. Based on the absorbance change in each solution, the amounts of **Ru-dpqpy** and **PtP-py** adsorbed over the individual FTO/TiO_2 electrode were estimated to be 0.12 and 0.10 μmol/cm^2, respectively.[44] The detailed studies using the FTO/TiO_2/**PtP-py** cathode unveiled its extremely small onset overpotential for HER, which is even smaller than 50 meV. Although it still adopts a precious element, the single-atom nature per catalyst clearly achieves drastically higher cost effectiveness. Thus, at the **PtP-py**-modified TiO_2 electrode, H_2 production proceeds spontaneously without the need for any additional external bias, in the same manner as observed when platinum was adopted at the cathode.[42] It must be noted here that the conduction band (CB) edge potential (i.e., flatband potential; E_{FB} = -0.40 -0.059pH V vs. SCE[45]) possesses a driving force for H_2 production larger than 50 meV (ca. 160 meV), which is somehow closely correlated with the driving force for the $MV^{+\bullet}$-driven HER at pH=5.0 (see above). We now postulate that the **PtP-py** anchored over the TiO_2 surfaces cannot take the advantage of the above-mentioned dimerization pathway in order to lower the activation barrier for the often rate-limiting hydride formation process. Actually, the ideal π-π stacking distances of aromatic systems are ca. 3.4 Å, which clearly causes steric blockage to have a sufficiently strong Pt-Pt association (e.g., 2.8-3.2 Å) between the **PtP-py** units. An important insight gained in our recent study on the photocatalytic CO_2 reduction by water-soluble cobalt porphyrins[46] seems relevant to the reason why the filled Pt d_{z2} electron pair in **PtP-py** can raise its basicity without the aid of metal-metal association. Our DFT-based mechanistic study on the cobalt porphyrins unveiled that the filled d_{z2} orbital gradually increases its basicity upon successive porphyrin-based reduction processes.[46] The injection of electrons into the vacant π* orbitals causes substantial congestion in the electron density surrounding the metal d orbitals, leading to cause the destabilization in some of the filled d orbitals. We thus speculate that the relatively low overpotential achieved by **PtP-py** is induced by the porphyrin-based reduction processes. The detailed study is now in progress.

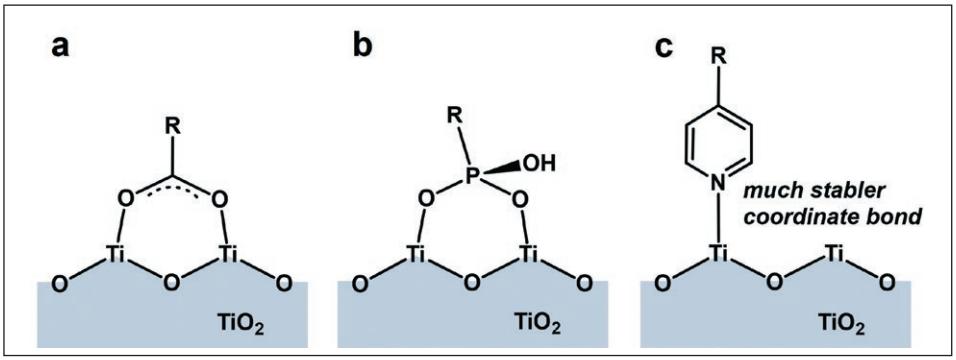

Figure 4. Schematic representations of possible binding modes for carboxylate (a), phosphonate (b), and pyridyl (c) anchors over the TiO_2 surfaces.

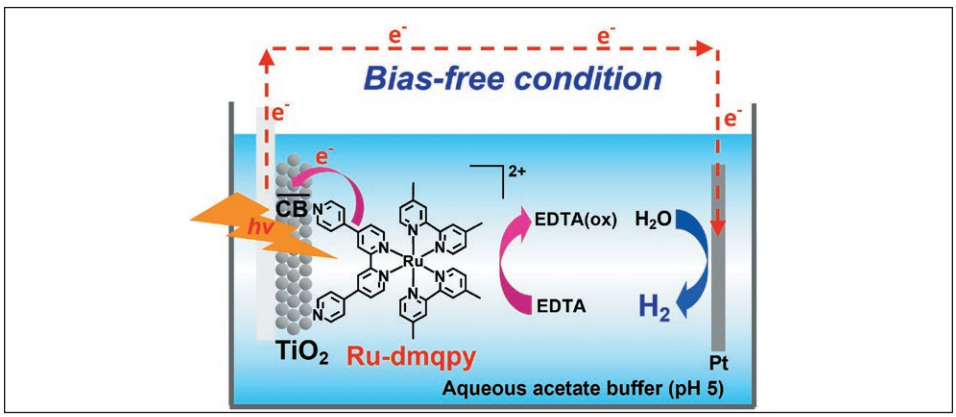

Figure 5. The FTO/TiO_2/Ru-dmqpy photoanode and a platinum electrode connected with a simple conductive wire, exhibiting its high stability and effectiveness in H_2 evolution at the dark cathode.[42]

Why electrons flow between the two electrodes with bias-free conditions?

To clarify the operation mechanism of our molecular-based PECs, linear potential sweep was made using a two-electrode configuration PEC made up of the FTO/TiO_2/**Ru-dpqpy** photoanode and FTO/TiO_2/**PtP-py** cathode.[44] Using this setup, the photoanode potential was scanned versus the cathode potential with the reference terminal short connected to the cathode. The measurement was also combined with the light-on and -off switching cycles (Figure 7a). Thus, the potential axis has a description of *V vs. cathode*. The measurements were carried out using an acetate buffer solution (0.1 M, pH 5.0) containing **Donor** (EDTA). Control experiments were also carried out by suppressing either **Ru-dpqpy** or **PtP-py** in electrodes. One of the most remarkable results is that the photocurrent density reaches ca. 0.4 mA/cm^2 even at 0 V vs. cathode, indicating that a sufficient current flows even with this bias-free condition (Figure 7a).[44] In addition, upon holding the anode potential at 0 V for 1 h with the light-on condition, ca. 4.2 μmol of H_2 evolved at the dark cathode with a near quantitative Faradaic efficiency. The results clearly indicated that electrons injected into the CB of TiO_2 at the photoanode flow over to the cathode even without applying any external bias. Indeed, even by the lack of **PtP-py** in the cathode, the FTO/TiO_2 cathode shows a color change into blue due to the substantial charge accumulation at the CB (Figure 7b,c). It was also confirmed that the electrons reaching the cathode can effectively drive the HER catalyzed by **PtP-py** with vigorous evolution of bubbles (Figure 7d,e). By disconnecting the electrochemical analyzer from the PEC, we further ascertained that a relatively small *photoinduced* potential shift is given between the two electrodes. The observed shift is rather small (ca. 20 μV) but certainly caused the electromotive force (EMF) required to transfer electrons from the photoanode to the cathode. The origin of EMF was further investigated by observing the charge accumulation into the CB at the photoanode by simply illuminating the FTO/TiO_2/**Ru-dpqpy** electrode soaked in the solution containing **Donor** (EDTA) (Figure 7f). The *in-situ* absorption spectroscopy clearly evidenced the growth of a broad visible to NIR band ascribable to the charge accumulation at the CB of TiO_2 (Figure 7f). The electron

filling into the CB causes a negative shift in the Fermi level of TiO_2, which is known as a Burstein-Moss shift. We thus concluded that the origin of EMF in our PEC arises from the upward shift in the Fermi level of TiO_2 at the photoanode, leading to promote the transfer of electrons to the cathode. This interpretation was further supported by the rational correlation between the H_2 evolution and the EMF (Figure 7g), for the rise in EMF (ca. 20 μV) and the H_2 production both concomitantly take place only within the light-on period (Figure 7g). These observations well rationalized the fact that the solar H_2 production occurs at the cathode even under bias-free conditions.

Splitting water by two TiO_2 electrodes anchored with molecular catalysts.

In spired by our previous finding in the water oxidation activity of cobalt porphyrins,[47] the anode *photochemically* driving water oxidation was initially designed to be given by co-adsorption of **Ru-dpqpy** (PS) and a cobalt porphyrin WOC possessing a pyridyl anchor (**CoP-py**; see Figure 8a). However, our study revealed that the FTO/TiO_2/**Ru-dpqpy**/**CoP-py** electrode does not show any desirable photocatalytic performance, which we assumed to be due to the lack of sufficient driving force for water oxidation when driven by the Ru(III)/Ru(II) couple of **Ru-dpqpy**. We thus postulated that the idealized PEC (Figure 3c) is only achievable with an appropriate choice of the PS having a sufficiently higher driving force for the water oxidation catalyzed by **CoP-py**, which is now in progress. In order to precisely understand the driving force required to promote the water oxidation by **CoP-py**, we decided to examine the electrolysis performance by the set of the FTO/TiO_2/**CoP-py** and FTO/TiO_2/**PtP-py** electrodes when adopted in water splitting in the dark (Figure 8).[48] As a result, this molecular-catalyst-anchored water electrolyzer was found to promote simultaneous generation of H_2 and O_2 in a 2:1 molar ratio with a nearly quantitative Faradaic efficiency. The electrocatalytic performances of the anode and cathode were separately examined as a function of pH using the standard three-electrode configuration electrochemical cell (Figure 8b). The cathode exhibited its pH-independent characteristics, consistent with the pH-dependent shift of the flatband potential (see above) which exactly coincides with that of the equilibrium potential for water reduction: $E(H_2/2H^+) = -0.059pH$. On the other hand, the anode showed a decrease in the onset overpotential with increasing pH, consistent with the shift in water oxidation potential: $E(H_2/2H^+) = 1.23-0.059pH$. The smallest onset potential was observed to be minimized at pH=9.0 with the value of ca. 1.00 V vs. SCE (i.e., 1.77 V vs. RHE), indicative of the onset overpotential of 540 meV for water oxidation with the **CoP-py**-anchored anode.

As for the **PtP-py**-anchored cathode, the onset potential for HER was observed to be located more positive than 0.83 V vs. SCE (i.e., -0.06 V vs. RHE) at pH=9.0, revealing that the onset overpotential is even smaller than 60 meV. We finally adopted a two-electrode configuration electrochemical cell by sweeping the anode potential versus the cathode potential which is shorted connected to the reference terminal. This setup allowed us to more clearly evaluate the water electrolysis performance of our TiO_2-electrode-based electrolyzer. The large current derived from overall water splitting was thus observed with the applied potential of 1.8 V (Figure 8c). The minimum overall potential required to trigger the water decomposition was determined as ca. 1.75 V by conducting the *in-situ* quantification of the H_2 and O_2 evolved under various applied potentials. The result indicated that our molecular-catalyst-anchored water electrolyzer start splitting water with addition of 520 meV or more to the theoretical potential (1230 meV). This overall required overpotential (520 meV) corresponds to the sum of driving forces required to drive the HER and OER. Interestingly, this value is even less than the sum of the values independently determined for the anode and cathode using the three-electrode system (600 meV; see above). During 1 h of controlled potential electrolysis (CPE) using the applied potential of 2.2 V vs. cathode, corresponding to ca. 1.0 V of applied overall overpotential, this water electrolyzer produced H_2 and O_2 in a 2:1 molar ratio (5.9 ± 0.8 and 3.1 ± 0.3 μmol, respectively) with a nearly quantitative Faradaic efficiency (90 ± 6% and 94 ± 4%, respectively) (Figure 8d). The TONs based on the amounts of **PtP-py** and **CoP-py** adsorbed over the individual FTO/TiO_2 electrode were estimated to be 59 ± 8 and 31 ± 3, respectively. An interesting observation for this water electrolyzer is that H_2 production continues to occur until satisfying the quantitative Faradaic efficiency even after stopping the 1 h of CPE, while such a delay response is not observed for O_2 production (Figure 8d). The delayed action in the cathode was rationally interpreted by the fact that the electrons transferred from the anode are once

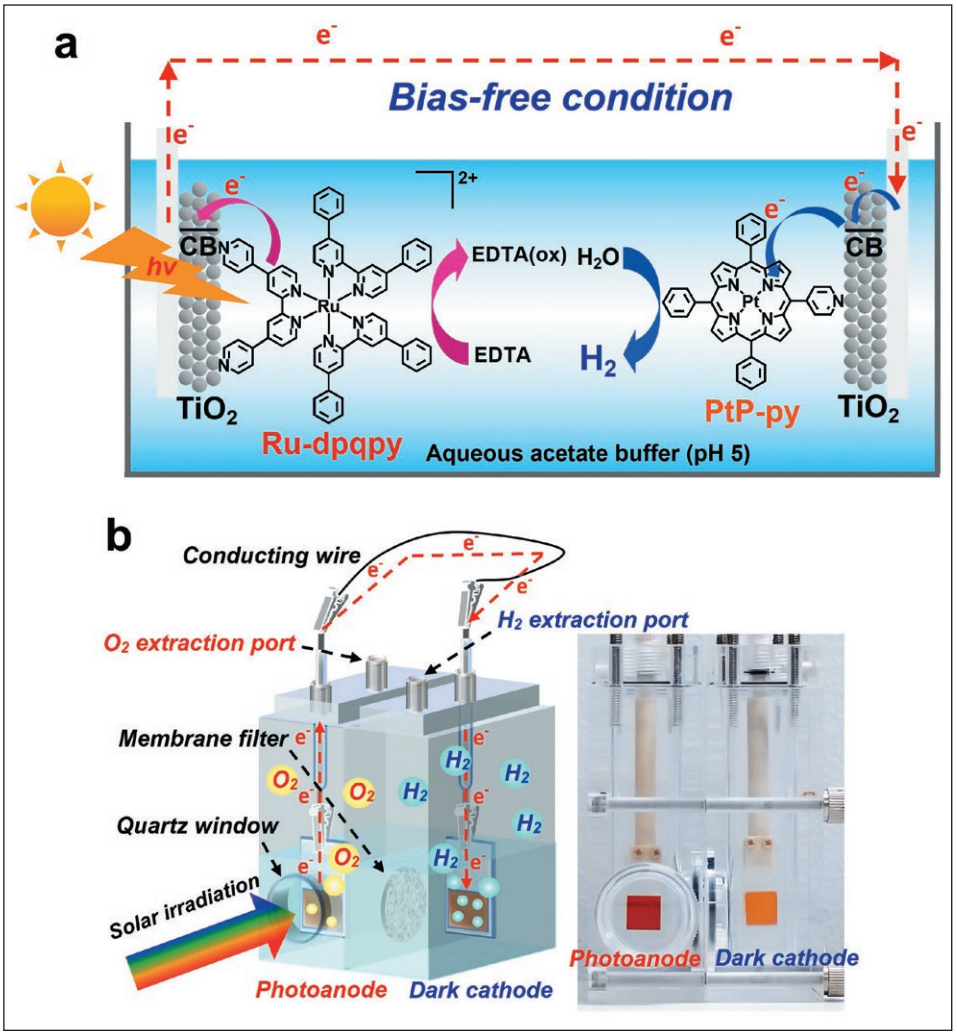

Figure 6. (a) Schematic representation of molecular-based PEC cell for solar H_2 production reported by authors' group.[43,44] (b) Schematic diagram and photograph of the molecular-based PEC consisting of the FTO/TiO_2/Ru-dpqpy photoanode and the FTO/TiO_2/PtP-py cathode.

charged into the CB in the cathode followed by their delayed consumption in the **PtP-py**-catalyzed HER. This behavior is clearly attributable to the uncontrollable nature of the driving force for the HER using the CB of TiO_2. We also confirmed that both **PtP-py** and **CoP-py** are intact for at least an hour under the above water electrolysis conditions. Thus, our study, for the first time, demonstrated that a molecular-catalyst-based water electrolyzer is achievable by employing the mesoporous TiO_2 films as the electrode materials on both anode and cathode. The band engineering enabling the fine tuning of the CB levels in both electrodes is considered as one of the important strategies towards the development of advanced technology for the solar hydrogen generation.

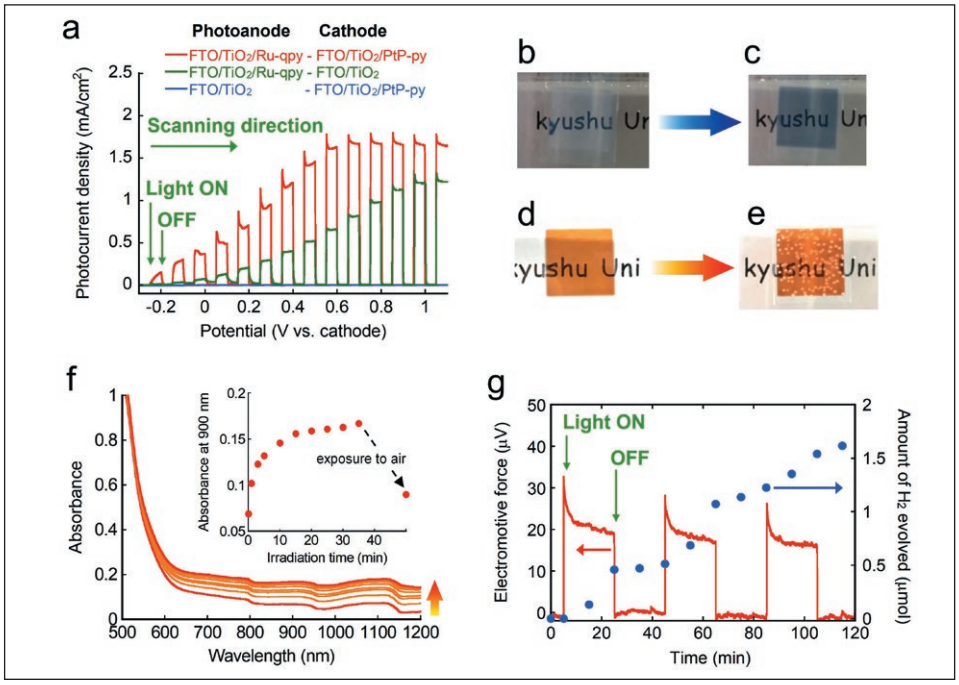

Figure 7. (a) Linear sweep voltammograms (LSV) for our PECs under intermittent irradiation (λ > 400 nm). Photographs of the FTO/TiO_2 and the FTO/TiO_2/PtP-py cathodes before (b,d) and after (c,e) the LSV measurements under irradiation condition. (f) Spectral changes during the visible light irradiation to the FTO/TiO_2/Ru-dpqpy electrode submerged into an acetate buffer solution containing 30 mM EDTA under Ar. (g) Time course of the EMF and the amount of H_2 evolved under intermittent irradiation.[44]

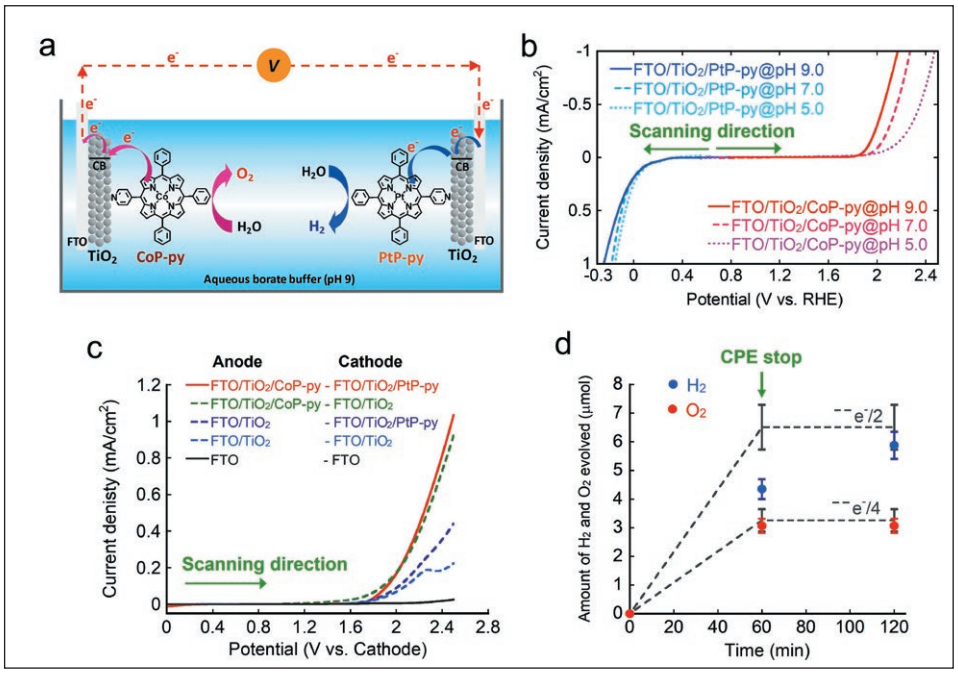

Figure 8. (a) Schematic representation of molecular-catalyst-anchored water electrolyzer consisting of the FTO/TiO_2/CoP-py anode and the FTO/TiO_2/PtP-py cathode (coverage of catalyst, 0.10 μmol/cm^2 for each). (b) The pH dependences in the LSVs measured for either the anode or cathode (100 mV/s). (c) LSVs with the cathode short connected to the reference terminal (0.1 M borate buffer, pH=9.0). (d) The H_2 and O_2 evolved over time during 1 h of electrolysis with the anode potential held at 2.2 V vs. cathode (pH=9.0), where the dashed line corresponds to the amount of each gas expected for the 100% Faradaic efficiency.[48]

Summary and Outlook

We have emphasized the importance of keep tackling to innovate the solar-driven hydrogen generation technology by appreciating rather highly advanced technology in the hydrogen fuel cells which are likely to offer a significant contribution to our future society because of their sufficiently high fuel-to-electricity conversion efficiency together with the high capacity enabling the large scale energy supply based on the storable high energy density fuels. In sharp contrast with the artificial fuel generation methods recently explored by other researchers, our fuel generation method is designed to avoid the gas separation facility together with the double photon pumping route to transfer one electron. These strategies intend to make our target photosynthetic devices amenable to produce the highest achievable energy on the basis of the solar light energy absorbed. Nature has somehow achieved such photosynthetic systems after repeating a few billion years of evolution processes. Nature does not evolve flammable fuels mixed with dioxygen by smartly converting their fuels into water-soluble as well as recognizable forms. The side product, that is, dioxygen is simply ejected from the organism. The chemical engineering features are thus well advanced in natural organisms. We notify that such chemical engineering part of research has not been well advanced in the field of artificial photosynthesis. The advanced studies on such issues are thus likely to open up a new avenue of research. In this review, we also discussed some of our successful advancement in getting deeper insights into the mechanisms of molecular catalysis related to energy conversion processes. Development of molecular-anchored photosynthetic systems largely relies on the knowledge gained from the basics studies on the small molecular systems. Since our ability to control the molecular catalytic properties is still quite limited, we should further advance our knowledge and artificial skills to finely control all the photochemical and electrochemical actions of the molecular systems in our hand. ◆

Acknowledgment

This work was supported by JSPS KAKENHI Grant Numbers JP16K05726, JP18H01996, JP18H05171, JP19K05502 and JP21H01952.

References

1. Staffell, I.; Scamman, D.; Abad, A.V.; Balcombe, P.; Dodds, P.E.; Ekins, P.; Shahd, N.; Warda, K.R. (2019). The Role of Hydrogen and Fuel Cells in the Global Energy System. Energy Environ. Sci. **12**, 463-491.
2. Alazemi, J.; Andrews, J. (2015). Automotive Hydrogen Fueling Stations: An International Review. Renewable Sustainable Energy Rev. **48**, 483-499.
3. Baldi, F.; Wang, L.; Pérez-Fortes, M.; Maréchal, F. (2019). A Cogeneration System Based on Solid Oxide and Proton Exchange Membrane Fuel Cells with Hybrid Storage for Off-Grid Applications. Front. Energy Res. **6**, 139.
4. Herraiz, L.; Lucquiaud, M.; Chalmers, H.; Gibbins, J. (2020). Sequential Combustion in Steam Methane Reformers for Hydrogen and Power Production with CCUS in Decarbonized Industrial Clusters. Front. Energy Res. **8**, 180.
5. Boretti, A.; Banik, B.K. (2021). Advances in Hydrogen Production from Natural Gas Reforming. Adv. Energy Sustainability Res. **2**, 2100097.
6. Tedsree, K.; Li, T.; Jones, S.; Chan, C.W.A.; Yu, K.M.K.; Bagot, P.A.J.; Marquis, E.M.; Smith, G.D.W.; Tsang, S.C.E. (2011). Hydrogen Production from Formic Acid Decomposition at Room Temperature Using a Ag–Pd Core–Shell Nanocatalyst. Nat. Nanotechnol. **6**, 302-307.
7. Parent, A.R.; Nakazono, T.; Tsubonouchi, Y.; Taira, N.; Sakai, K. (2019). Mechanisms of Water Oxidation Using Ruthenium, Cobalt, Copper, and Iron Molecular Catalysts. Adv. Inorg. Chem. **74**, 197-240.
8. Nishiyama, H.; Yamada, T.; Nakabayashi, M.; Maehara, Y.; Yamaguchi, M.; Kuromiya, Y.; Nagatsuma, Y.; Tokudome, H.; Akiyama, S.; Watanabe, T.; Narushima, R.; Okunaka, S.; Shibata, N.; Takata, T.; Hisatomi, T.; Domen, K. (2021). Photocatalytic Solar Hydrogen Production from Water on a 100-m^2 Scale. Nature **598**, 304-307.
9. Iguchi, M.; Himeda, Y.; Manaka, Y.; Kawanami, H. (2016). Development of an Iridium-Based Catalyst for High-Pressure Evolution of Hydrogen from Formic Acid. ChemSusChem **9**, 2749-2753.
10. Zhong, H.; Iguchi, M.; Song, F.-Z.; Chatterjee, M.; Ishizaka, T.; Nagao, I.; Xu, Q.; Kawanami, H. (2017). Automatic High-Pressure Hydrogen Generation from Formic Acid in the Presence of Nano-Pd Heterogeneous Catalysts at Mild Temperatures. Sustainable Energy Fuels **1**, 1049-1055.
11. Fujishima, A.; Honda, K. (1972). Electrochemical Photolysis of Water at a Semiconductor Electrode. Nature **238**, 37-38.
12. Kirch, M.; Lehn, J.-M.; Sauvage, J.-P. (1979). Hydrogen Generation by Visible Light Irradiation of Aqueous Solutions of Metal Complexes. An Approach to the Photochemical Conversion and Storage of Solar Energy. Helv. Chim. Acta **62**, 1345-1384.
13. Esswein, A.J.; Nocera, D.G. (2007). Hydrogen Production by Molecular Photocatalysis. Chem. Rev. **107**, 4022-4047.
14. Fukuzumi, S.; Yamada, Y.; Suenobu, T.; Ohkubo, K.; Kotani, H. (2011). Catalytic Mechanisms of Hydrogen Evolution with Homogeneous and Heterogeneous Catalysts. Energy Environ. Sci. **4**, 2754-2766.
15. Artero, V.; Chavarot-Kerlidou, M.; Fontecave, M. (2011). Splitting Water with Cobalt. Angew. Chem. Int. Ed. **50**, 7238-7266.
16. Dalle, K.E.; Warnan, J.; Leung, J.J.; Reuillard, B.; Karmel, I.S.; Reisner, E. (2019). Electro- and Solar-Driven Fuel Synthesis with First Row Transition Metal Complexes. Chem. Rev. **119**, 2752-2875.
17. Sakai, K.; Ozawa, H. (2007). Homogeneous Catalysis of Platinum(II) Complexes in Photochemical Hydrogen Production from Water. Coord. Chem. Rev. **251**, 2753-2766.
18. Sakai, K.; Matsumoto, K. (1988). Photochemical Reduction of Water to Hydrogen Catalyzed by Mixed-Valent Tetranuclear Platinum Complex. J. Coord. Chem. **18**, 169-172.
19. Sakai, K.; Matsumoto, K. (1990). Homogeneous Catalysis of Platinum Blue Related Complexes in Photoreduction of Water into Hydrogen. J. Mol. Catal. **62**, 1-14.
20. Sakai, K.; Kizaki, Y.; Tsubomura, T.; Matsumoto, K. (1993). Homogeneous Catalysis of Mixed-Valent Octanuclear Platinum Complexes in Photochemical Hydrogen Production from Water. J. Mol. Catal. **79**, 141-152.
21. Tanaka, S.; Masaoka, S.; Yamauchi, K.; Annaka, M.; Sakai, K. (2010). Photochemical and Thermal Hydrogen Production from Water Catalyzed by Carboxylate-Bridged Dirhodium(II) Complexes. Dalton Trans. **39**, 11218-11226.
22. Kawano, K.; Yamauchi, K.; Sakai, K. (2014). A Cobalt-NHC Complex as an Improved Catalyst for Photochemical Hydrogen Evolution from Water. Chem. Commun. **50**, 9872-9875.
23. Sakai, K.; Tanaka, Y.; Tsuchiya, Y.; Hirata, K.; Tsubomura, T.; Iijima, S.; Bhattacharjee, A. (1998). New Structural Aspects of α-Pyrrolidinonate-Bridged and α-Pyridonate-Bridged, Homo- and Mixed-Valence, Di- and Tetranuclear *cis*-Diammineplatinum Complexes: Eight New Crystal Structures, Stoichiometric 1:1 Mixture of $Pt(2.25+)_4$ and $Pt(2.5+)_4$, New Quasi-One-Dimensional Halide-Bridged $[Pt(2.5+)_4\text{-}Cl\cdots]_\infty$ System, and Consideration for Solution Properties. J. Am. Chem. Soc. **120**, 8366-8379.
24. Ozawa, H.; Haga, M.; Sakai, K. (2006). A Photo-Hydrogen-Evolving Molecular Device Driving Visible-Light-Induced EDTA-Reduction of Water into Molecular Hydrogen. J. Am. Chem. Soc. **128**, 4926-4927.
25. Yamauchi, K.; Masaoka, S.; Sakai, K. (2009). Evidence for Pt(II)-Based Molecular Catalysis in the Thermal Reduction of Water into Molecular Hydrogen. J. Am. Chem. Soc. **131**, 8404-8406.
26. Ogawa, M.; Ajayakumar, G.; Masaoka, S.; Kraatz, H.-B.; Sakai, K. (2011). Platinum(II)-Based Hydrogen-Evolving Catalysts Linked to Multipendant Viologen Acceptors: Experimental and DFT Indications for Bimolecular Pathways. Chem. Eur. J. **17**, 1148-1162.
27. Ozawa, H.; Sakai, K. (2011). Photo-Hydrogen-Evolving Molecular Devices Driving Visible-Light-Induced Water Reduction into Molecular Hydrogen: Structure-Activity Relationship and Reaction Mechanism. Chem. Commun. **47**, 2227-2242.
28. Rabbani, R.; Saeedi, S.; Nazimuddin, M.; Barbero, H.; Kyritsakas, N.; White, T.A.; Masson, E. (2021). Enhanced Photoreduction of Water Catalyzed by a Cucurbit[8]uril-Secured Platinum Dimer. Chem. Sci. **12**, 15347-15352, and references therein.
29. Kobayashi, M.; Masaoka, S.; Sakai, K. (2011). Photoinduced Hydrogen Evolution from Water Based on a Z-Scheme Photosynthesis by a Simple Platinum(II) Terpyridine Derivative. Angew. Chem. Int. Ed. **51**, 7431-7434.
30. Kitamoto, K.; Sakai, K. (2014). Pigment-Acceptor-Catalyst Triads for Photochemical Hydrogen Evolution. Angew. Chem. Int. Ed. **53**, 4618-4622.
31. Suneesh, C.V.; Balan, B.; Ozawa, H.; Nakamura, Y.; Katayama, T.; Muramatsu, M.; Nagasawa, Y.; Miyasaka, H.; Sakai, K. (2014). Mechanistic Studies of Photoinduced Intramolecular and Intermolecular Electron Transfer Processes in RuPt-Centred Photo-Hydrogen-Evolving Molecular Devices. Phys. Chem. Chem. Phys. **16**, 1607-1616.
32. Lin, S.; Kitamoto, K.; Ozawa, H.; Sakai, K. (2016). Improved Photocatalytic Hydrogen Evolution Driven by Chloro(terpyridine)platinum(II) Derivatives Tethered to a Single Pendant Viologen Acceptor. Dalton Trans. **45**, 10643-10654.
33. Kitamoto, K.; Sakai, K. (2016). Photochemical H_2 Evolution from Water Catalyzed by Dichloro(diphenylbipyridine)platinum(II) Derivative Tethered to Multiple Viologen Acceptors. Chem. Commun. **52**, 1385-1388.
34. Ashford, D.L.; Gish, M.K.; Vannucci, A.K.; Brennaman, M.K.; Templeton, J.L.; Papanikolas, J.M.; Meyer, T.J. (2015). Molecular Chromophore-Catalyst Assemblies for Solar Fuel Applications. Chem. Rev. **115**, 13006-13049.
35. Wang, M.; Yang, Y.; Shen, J.; Jiang, J.; Sun, L. (2017). Visible-Light-Absorbing Semiconductor/Molecular Catalyst Hybrid Photoelectrodes for H_2 or O_2 Evolution: Recent Advances and Challenges. Sustainable Energy Fuels **1**, 1641-1663.
36. Shan, B.; Brennaman, M.K.; Troian-Gautier, L.; Liu, Y.; Nayak, A.; Klug, C.M.; Li, T.T.; Bullock, R.M.; Meyer, T.J. (2019). A Silicon-Based Heterojunction Integrated with a Molecular Excited State in a Water-Splitting Tandem Cell. J. Am. Chem. Soc. **141**, 10390-10398.
37. Gong, L.; Zhang, P.; Liu, G.; Shan, Y.; Wang, M. (2021). A Silicon-Based Hybrid Photocathode Modified with an N_5-Chelated Nickel Catalyst in a Noble-Metal-Free Biomimetic Photoelectrochemical Cell for Solar-Driven Unbiased Overall Water Splitting J. Mater. Chem. A **9**, 12140-12151.
38. Ozawa, H.; Sugiura, T.; Kuroda, T.; Nozawa, K.; Arakawa, H. (2016). Highly Efficient Dye-Sensitized Solar Cell Based on a Ruthenium Sensitizer Bearing a Hexylthiophene Modified Terpyridine Ligand. J. Mater. Chem. A **4**, 1762-1770.
39. Ito, S.; Liska, P.; Comte, P.; Charvet, R.; Péchy, P.; Bach, U.; Schmidt-Mende, R.; Zakeeruddin, S.M.; Kay, A.; Nazeeruddina, M.K.; Grätzel, M. (2005). Control of Dark Current in Photoelectrochemical ($TiO_2/I^-\text{-}I_3^-$) and Dye-Sensitized Solar Cells. Chem. Commun. **2005**, 4351-4353.
40. Brewster, T.P.; Konezny, S.J.; Sheehan, S.W.; Martini, L.A.; Schmuttenmaer, C.A.; Batista, V.S.; Crabtree, R.H. (2013). Hydroxamate Anchors for Improved Photoconversion in Dye-Sensitized Solar Cells. Inorg. Chem. **52**, 6752–6764.
41. Shibayama, N.; Ozawa, H.; Abe, M.; Ooyama, Y.; Arakawa, H. (2014). A New Cosensitization Method Using the Lewis Acid Sites of a TiO_2 Photoelectrode for Dye-Sensitized Solar Cells. Chem. Commun. **50**, 6398-6401.
42. Takijiri, K.; Morita, K.; Nakazono, T.; Sakai, K.; Ozawa, H. (2017). Highly Stable Chemisorption of Dyes with Pyridyl Anchors Over TiO_2: Application in Dye-Sensitized Photoelectrochemical Water Reduction in Aqueous Media. Chem. Commun. **53**, 3042-3045.
43. Morita, K.; Takijiri, K.; Sakai, K.; Ozawa, H. (2017). A Platinum Porphyrin Modified TiO_2 Electrode for Photoelectrochemical Hydrogen Production from Neutral Water Driven by the Conduction Band Edge Potential of TiO_2. Dalton Trans. **46**, 15181-15185.
44. Morita, K.; Sakai, K.; Ozawa, H. (2019). A New Class of Molecular-Based Photoelectrochemical Cell for Solar Hydrogen Production Consisting of Two Mesoporous TiO_2 Electrodes. ACS Appl. Energy Mater. **2**, 987-992.
45. Boschloo, G.; Fitzmaurice, D. (2000). Electron Accumulation in Nanostructured TiO_2 (Anatase) Electrodes. J. Electrochem. Soc. **147**, 1117-1123.
46. Zhang, X.; Yamauchi, K.; Sakai, K. (2021). Earth-Abundant Photocatalytic CO_2 Reduction by Multielectron Chargeable Cobalt Porphyrin Catalysts: High CO/H_2 Selectivity in Water Based on Phase Mismatch in Frontier MO Association. ACS Catal. **11**, 10436-10449.
47. Nakazono, T.; Sakai, K. (2016). Improving the Robustness of Cobalt Porphyrin Water Oxidation Catalysts by Chlorination of Aryl Groups. Dalton Trans. **45**, 12649-12652.
48. Akamine, K.; Morita, K.; Sakai, K.; Ozawa, H. (2020). A Molecular-Based Water Electrolyzer Consisting of Two Mesoporous TiO_2 Electrodes Modified with Metalloporphyrin Molecular Catalysts Showing a Quantitative Faradaic Efficiency. ACS Appl. Energy Mater. **3**, 4860-4866.